

## Fundamental Reflectivity and Band Structure of ZnTe, CdTe, and HgTe

MANUEL CARDONA

RCA Laboratories, Princeton, New Jersey

AND

D. L. GREENAWAY

Laboratories RCA Ltd., Zurich, Switzerland

(Received 20 February 1963)

The fundamental reflectivity of ZnTe, CdTe, and HgTe has been measured over the energy range 1.0–25 eV at room temperature and 1.0–6.5 eV at 77°K. Corners and maxima in the reflectivity are identified with interband transitions at the symmetry points  $\Gamma$ ,  $L$ , and  $X$  and in the  $[111]$  direction inside the Brillouin zone. At about 12 eV the reflection spectrum of these and other II-VI compounds shows structure which has been assigned to transitions from  $d$ -electron levels in the metal to the conduction band. The systematics of the band structure of zincblende-type compounds is discussed. Several rules are given for calculating effective masses in these and related materials.

### INTRODUCTION

MEASUREMENT of reflectivity in the fundamental absorption region of a semiconductor provides a direct and simple method of observing strong interband transitions and studying the band structure of the material. Because of the high absorption coefficient in the fundamental region, transmission measurements at short wavelengths require elaborate and often rather tedious techniques to prepare suitable specimens. Considerable attention has recently been given to evaluating the reflectivity spectra of the diamond and zincblende semiconductors.<sup>1–6</sup> The marked similarities between all these spectra, coupled with the considerable amount of other information available on the elemental semiconductors silicon and germanium, have made it possible to give a very reasonable interpretation of the experimental results. Recent pseudopotential band structure calculations on germanium,<sup>7</sup> and silicon,<sup>8</sup> and some low-temperature reflectivity results on III-V compounds,<sup>9</sup> lend further support to the general picture. The work reported here is the result of more detailed measurements than have been made previously on the group II-VI zincblende materials ZnTe, CdTe, and HgTe.<sup>5</sup> The reflectivity curves have been obtained over the range 1.0–25 eV at room temperature and 1.0–6.5 eV at 77°K. An account is given of the precautions which must be taken to obtain reliable reflectivity curves at low temperature. These spectra are interpreted in terms of the band structure of the compounds along the lines

followed for the interpretation of the reflection of the Group IV and III-V materials. The structure observed for these and other II-VI materials around 12 eV is assigned to transitions from the  $d$  electrons of the Group II atom to the conduction band.

### METHOD OF MEASUREMENT

#### A. Equipment

The reflectivity of evaporated aluminum mirrors, though uniformly high in the infrared, falls off steeply towards the ultraviolet region of the spectrum. The ultraviolet reflectivity can be enhanced considerably by coating with MgF<sub>2</sub> or LiF, but uniformity over a wide spectral region cannot be easily obtained. Moreover, the reflectivity of evaporated aluminum can suffer from serious aging effects. Therefore, for the measurement of the relatively weak structure associated with the fundamental reflectivity of many semiconductors, it is dangerous to use a calibrated reference mirror. The measurements reported here are all "absolute": No reference mirror and only one detector was used. The detector is moved from the position in which it measures the incident light intensity  $I_0$ , with the sample removed from the beam, to that in which it measures the reflected intensity  $I$ . A 500-mm Bausch and Lomb grating monochromator was used in the measurements below 6.5 eV and a 1-meter Jarrell-Ash vacuum-ultraviolet spectrometer at higher photon energies. Two different sources were used for the vacuum spectrometer.<sup>10,11</sup> Up to 13 eV we used a high-voltage discharge in hydrogen produced by a Tanaka source. This source was also used with neon and helium to produce lines at 16.9 and 21.2 eV, respectively. In the region between 13 and 25 eV several discrete emission lines of argon were also obtained with the tube shown in Fig. 1. This tube, a modified version of that used by Ehrenreich and Philipp,<sup>10</sup> was operated at low voltage ( $\sim 100$  V), high current ( $\sim 2$  A), and low pressure ( $\sim 5 \times 10^{-2}$  mm of

<sup>1</sup> H. R. Philipp and E. A. Taft, Phys. Rev. **113**, 1002 (1959).

<sup>2</sup> M. Cardona and H. S. Sommers, Jr., Phys. Rev. **122**, 1382 (1961).

<sup>3</sup> J. Tauc and A. Abraham, in *Proceedings of the International Conference on Semiconductors Physics, 1960* (Czechoslovakian Academy of Sciences, Prague, 1961), p. 375.

<sup>4</sup> H. R. Philipp and E. A. Taft, Phys. Rev. **120**, 37 (1960).

<sup>5</sup> M. Cardona, Suppl. J. Appl. Phys. **32**, 2151 (1961).

<sup>6</sup> M. Cardona and D. L. Greenaway, Phys. Rev. **125**, 1291 (1962).

<sup>7</sup> D. Brust, J. C. Phillips, and F. Bassani, Phys. Rev. Letters **9**, 94 (1962).

<sup>8</sup> D. Brust, M. L. Cohen, and J. C. Phillips, Phys. Rev. Letters **9**, 389 (1962).

<sup>9</sup> D. L. Greenaway, Phys. Rev. Letters **9**, 97 (1962).

<sup>10</sup> H. Ehrenreich and H. R. Philipp, Phys. Rev. **129**, 1550 (1963).

<sup>11</sup> M. Cardona, Phys. Rev. **129**, 69 (1963).

mercury). The ionization of the argon was produced by means of the electron emission from a heated thoriated-tungsten cathode

Room-temperature reflectivity measurements are straightforward, but precautions must be taken to prevent film formation on the specimen surface at low temperatures. If such formation occurs, these films produce effects that are irreproducible, and can radically alter the reflection characteristics of a surface. We have found that there are at least four causes which all produce these contaminating films: (a) poor vacuum (i.e., worse than  $10^{-4}$  mm of mercury), (b) inefficient cold trapping and consequent distillation of diffusion pump oil into the cryostat, (c) either the silicone or mineral vacuum grease commonly used on O-rings seals, (d) a volatile component which comes from Neoprene O-rings and will condense on any nearby cold surface. In the vacuum system used here, the cryostat is not filled with liquid nitrogen until the pressure is lower than  $10^{-5}$  mm of mercury. Cause (b) is eliminated by having two liquid-nitrogen traps between the diffusion pump and cryostat. (c) is eliminated by using ungreased O-rings throughout the system. Cause (d) is avoided by ensuring that there are no O rings near the cold part of the cryostat. Some improvement is also obtained by using Viton instead of Neoprene rings.<sup>12</sup> In the cryostat used with the Bausch and Lomb spectrometer, the two quartz windows were waxed in position using hard vacuum wax (Apiezon) which has an extremely low vapor pressure. Low-temperature reflectivity curves taken under these conditions still showed slight evidence of film formation, but the effect was limited to changes of less than 1% in sample reflectivity over a period of 1 h.

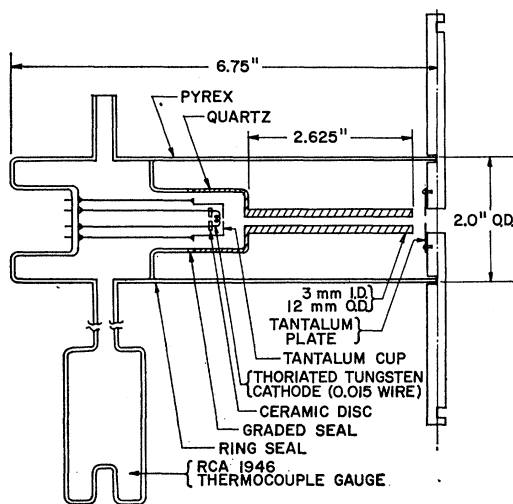


FIG. 1. Vacuum ultraviolet source.

<sup>12</sup> We are indebted to Dr. R. R. Addiss for suggesting the use of Viton rings.

## B. Sample Preparation

Attempts to etch samples of the three tellurides using a variety of standard semiconductor etchants were not very successful, resulting in reflectivity curves that were not reproducible. Consequently, all measurements reported here were made on cleaved, essentially single-crystal specimens. Due to the difficulty of finding large enough optically flat cleavage surfaces (particularly in HgTe), the absolute values of reflectivities shown on the experimental curves, must be regarded as approximate and may be subject to an error of  $\pm 10\%$ . The cleaved surfaces of all three materials appeared to be quite stable, and no significant changes were noticed over a period of weeks, though there were small differences between specimens of the same material

## RESULTS

The reflectivity curves for ZnTe, CdTe, and HgTe at room temperature and 77°K, for photon energies up to 6.5 eV, are shown in Fig. 2-4. The positions of the three principal maxima ( $E_1$ ,  $E_1 + \Delta_1$ , and  $E_2$ ) were reproducible to  $\pm 0.02$  eV or better, and were located accurately using detailed measurements (not shown here) over small spectral regions. The position of the split-off peak on the high-energy side of the  $E_2$  HgTe maximum varied from specimen to specimen; therefore, it may be subject to an error of  $\pm 0.05$  eV. The weak structure at  $e_1$ ,  $e_1 + \Delta_1$ ,  $E_0$ ,  $E_0 + \Delta_0$ , and  $E_0$  was not visible in every specimen, although when it appeared, the position in energy was reproducible; the visibility of these very

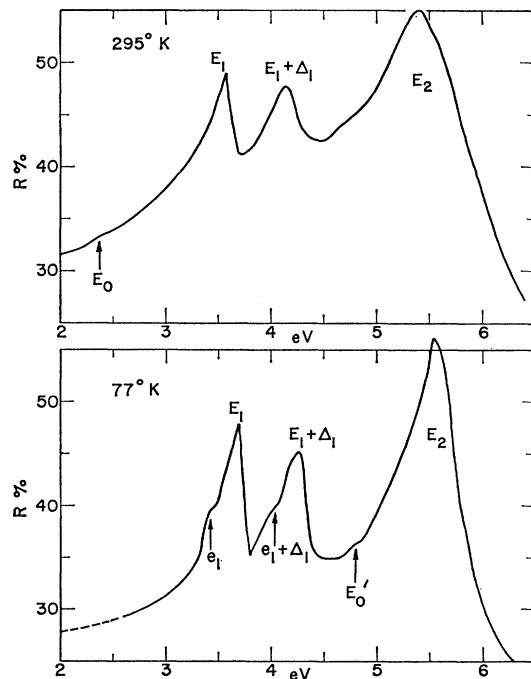


FIG. 2. Reflectivity of ZnTe at room temperature and 77°K.

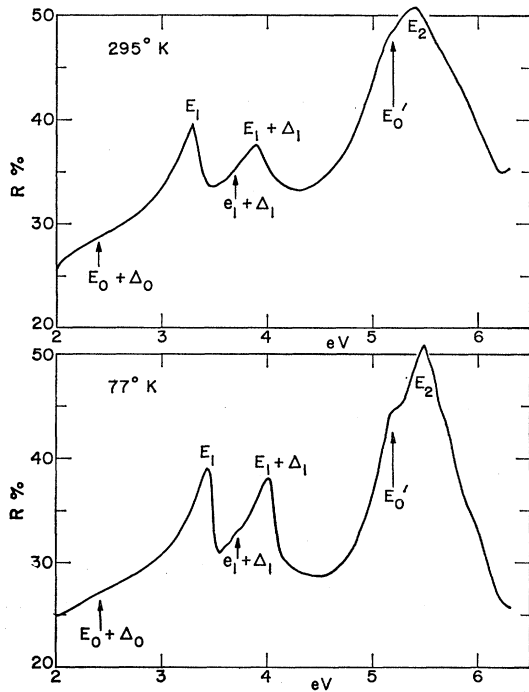


FIG. 3. Reflectivity of CdTe at room temperature and 77°K.

weak peaks is thus presumably critically dependent on the condition of the crystal surface and the quality of the crystal. The position of all the experimental reflectivity peaks is shown in Table I. The interpretation of the various peaks is discussed in Sec. IV. Estimates of the temperature coefficients of the maxima are also given; these coefficients were all estimated solely from the shift in energy between room- and liquid-nitrogen temperature.

Figure 5 shows the reflectivity of ZnTe, CdTe, and HgTe between 6 and 25 eV at room temperature. Four

TABLE I. Summary of experimental data.

	ZnTe		CdTe		HgTe	
	RT	77°K	RT	77°K	RT	77°K
$\Gamma_{15}-\Gamma_1$	$\left\{ \begin{array}{l} E_0+\Delta_0 \\ E_1 \end{array} \right.$	2.35 2.37 <sup>a</sup>	2.4 1.59 <sup>b</sup>	2.4 2.4	2.09	2.21
$\Lambda_3-\Lambda_1$	$\left\{ \begin{array}{l} E_1 \\ E_1+\Delta_1 \end{array} \right.$	3.58 3.71	3.32 3.44	3.32 3.44	2.71	2.85
$L_3-L_1$	$\left\{ \begin{array}{l} e_1 \\ e_1+\Delta_1 \end{array} \right.$	3.41 3.48	...	...	...	2.00
$\Gamma_{15}-\Gamma_{15}$	$\left\{ \begin{array}{l} (E_0') \\ (E_2) \end{array} \right.$	3.96 <sup>c</sup> 4.05	3.63 3.77	2.53	2.67	4.10
$X_5-X_1$		...	5.16 <sup>c</sup> 5.20	4.03	4.95	4.95
$X_5-X_3$		...	5.40 5.49	4.84	5.15	5.15
$L_3-L_3$	$\left\{ \begin{array}{l} E_1' \\ E_1'+\Delta_1 \end{array} \right.$	6.90 ...	6.76 ...	5.27 ± 0.05	6.55	...
$d_1$		7.49 ...	7.64 ...	7.80	7.80	...
$d_2$		10.6 ...	10.1 ...	9.7	9.7	...
		14.6 ...	13.8 ...	11.3	11.3	...
Temp. coefficients [10 <sup>-4</sup> eV/°C]						
$\Lambda_3-\Lambda_1$	$\left\{ \begin{array}{l} E_1 \\ E_1+\Delta_1 \end{array} \right.$	-6.0	-5.5	-6.0	-6.4	-6.4
$\Gamma_{15}-\Gamma_{15}$		-6.4	?	?	?	?
$X_5-X_1$		-6.0	-4.1	-5.1	-5.1	-5.1
$X_5-X_3$		?	?	-6.0	-6.0	-6.0

<sup>a</sup> E. Loh and R. Newman, J. Phys. Chem Solids 21, 3271 (1961).<sup>b</sup> D. G. Thomas, Suppl. J. Appl. Phys. 32, 2298 (1961).<sup>c</sup> Measured on a different specimen to that of Fig. 2.

peaks, labeled  $E_1'$ ,  $E_1'+\Delta_1$ ,  $d_1$ , and  $d_2$ , are seen for all three compounds. Their energies are also listed in Table I.

#### INTERPRETATION OF THE REFLECTIVITY PEAKS

The reflectivity spectra found for ZnTe, CdTe, and HgTe are very similar to those found for other zincblende- and diamond-structure materials.<sup>1-10</sup> By analogy with the other materials of the same family, we interpret the main  $E_2$  reflectivity maximum as due to transitions at the  $X$  point of the Brillouin zone (edge of zone in the

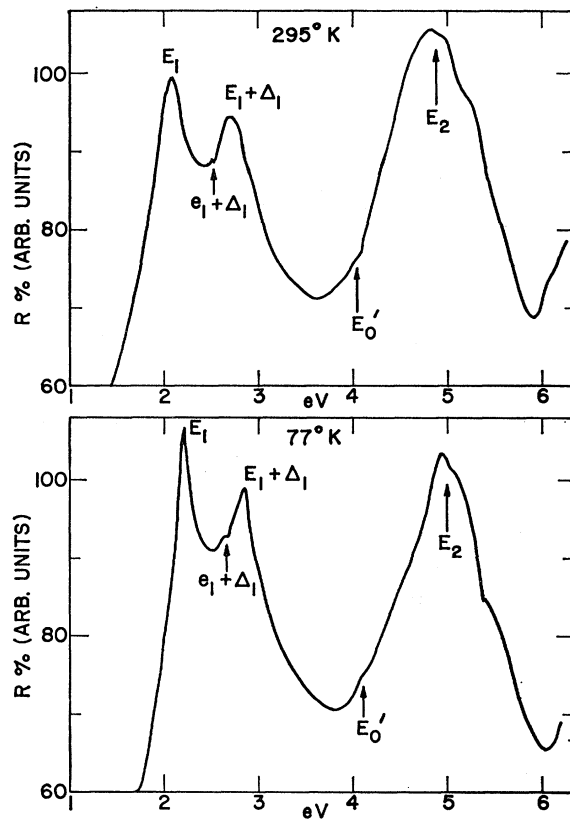


FIG. 4. Reflectivity of HgTe at room temperature and 77°K (in arbitrary units).

[100] direction), possibly combined with transitions to a saddle point in the [110] direction as indicated by the calculations of Brust *et al.*<sup>7</sup> for germanium. The  $X_1-X_3$  splitting seems to be smaller in HgTe than in CdTe. A decrease in the  $X_1-X_3$  splitting with increasing atomic number, attributable to a decrease in the polarity of the binding, has also been reported for other families of compounds with zincblende structure.<sup>11</sup> There is no experimental evidence of the  $X_1-X_3$  splitting in ZnTe; this splitting could be outside the energy range of our low-temperature measurements. The temperature coefficient of the  $X$  peak ( $-5 \times 10^{-4}$  eV°C<sup>-1</sup>) is much larger than the coefficients for the same peaks in germanium

and silicon ( $-2$  and  $0.6 \times 10^{-4} \text{ eV}^\circ\text{C}^{-1}$ , respectively<sup>2,13</sup>). This fact can be attributed to the degeneracy of the  $X_1$  state in the diamond-type materials.<sup>2</sup>

A very pronounced peak ( $E_0'$ ) appears at  $77^\circ\text{K}$  in CdTe on the low-energy side of the  $E_2$  peak at  $5.20 \text{ eV}$ . This peak shifts to  $5.16 \text{ eV}$  at room temperature. The small temperature coefficient of this peak ( $-2 \times 10^{-4} \text{ eV}^\circ\text{C}^{-1}$ ) suggests the assignment of this peak to transitions at  $k=0$  between the top of the valence band ( $\Gamma_{15}$ ) and the  $\Gamma_{15}$  conduction band.<sup>14</sup> Such transitions are readily observable in Si and in GaP and are also characterized by a similar temperature coefficient.<sup>6</sup> We have also assigned to these transitions the weak  $E_0'$  peaks observed in ZnTe at  $4.82 \text{ eV}$  and in HgTe at  $4.10 \text{ eV}$ . The discussion in the next section confirms this interpretation.

A weak peak can also be seen at  $77^\circ\text{K}$  on the high-energy side of the  $E_2$  peak for CdTe and HgTe. This peak occurs at  $5.15 \text{ eV}$  in HgTe and  $5.7 \text{ eV}$  in CdTe. This peak, which seems to be split from the  $X_5-X_1$  peak, has been attributed by Segall<sup>15</sup> to the spin-orbit splittings of the  $X_5$  point. In order to calculate the spin-orbit splittings at this point, the splittings of the constituent atoms must be subtracted instead of added. The value at  $X_5$  of the spin-orbit splitting, higher for CdTe than for HgTe, and in good agreement with the experimental observation reported here, can thus be estimated.

The low-energy  $E_1$  reflectivity doublet in germanium has been assigned by Brust *et al.*<sup>7</sup> to  $\Delta_3-\Delta_1$  transitions, at the  $[0.17, 0.17, 0.17]$  point of the Brillouin zone, the doublet structure being due to the spin-orbit splitting of the valence band. The former  $L$ -point assignment (edge of zone  $[111]$  direction) of these transitions in germanium had to be modified to agree with the results of the pseudopotential band structure calculation; according to this calculation the real  $L$ -point transitions should be much weaker than the  $\Delta$ -point transitions, and occur at slightly lower energies (approx.  $0.2 \text{ eV}$  lower than  $\Delta$ ). The spin-orbit splitting of the valence band is identical at  $\Delta$  and  $L$ . There is some experimental evidence in favor of the  $\Delta$  interpretation from the optical measurements of Marple and Ehrenreich<sup>16</sup> in germanium at  $25^\circ\text{K}$ , and from the reflectivity of GaAs at  $77^\circ\text{K}$ .<sup>9</sup> More conclusive evidence comes from the reflectivity of ZnTe shown in Fig. 2. This clearly shows two weaker thresholds at energies slightly lower than the  $E_1$  doublet components ( $e_1$  and  $e_1+\Delta_1$ ). These thresholds are resolved at room temperature, and exhibit the same temperature dependence as the main  $E_1$  peaks. The  $e_1$  and  $e_1+\Delta_1$  thresholds appear to be partially resolved in

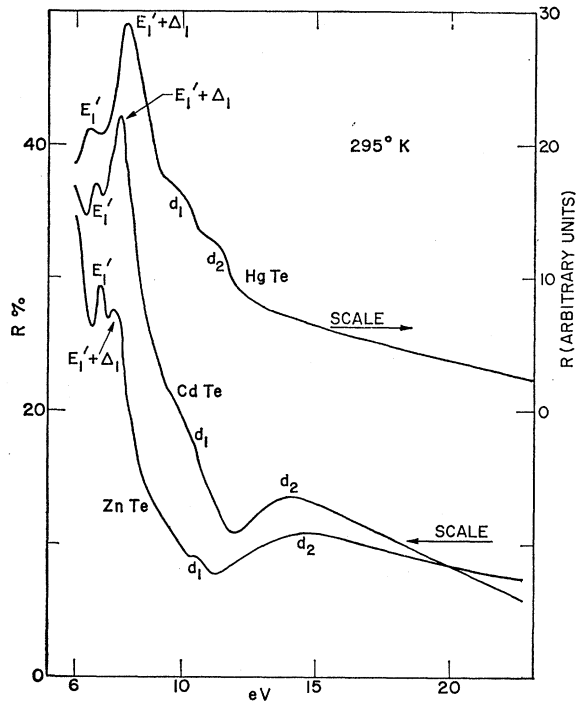


FIG. 5. Room-temperature reflectivity of HgTe, CdTe, and ZnTe between 6 and 25 eV.

HgTe, but only  $e_1 + \Delta_1$  has been observed in CdTe. The structure labeled  $E_0$  and  $E_0 + \Delta_0$  in Figs. 2 and 3 can be attributed to transitions at  $k=0$  from the highest valence band ( $\Gamma_{15}$ ) to the lowest conduction band ( $\Gamma_1$ ). The splitting  $\Delta_0 = 0.9 \text{ eV}$  obtained for ZnTe agrees well with three-halves of the splitting at  $L$  ( $\Delta_1 = 0.57 \text{ eV}$ ) and with estimates from the atomic splittings.<sup>5</sup> By comparing the energy found for the  $E_0 + \Delta_0$  peak in CdTe to the value of  $E_0$  found by other authors<sup>17</sup> we get  $\Delta_0 = 0.81$ , also approximately equal to three-halves of  $E_1$ .

The  $E_1'$  and  $E_1' + \Delta_1$  peaks shown in Fig. 5 have been assigned to transitions between the highest valence band at the  $L$  point ( $L_3$ ) and the  $L_3$  conduction band. This assignment is straightforward in ZnTe since one finds for these peaks the splitting  $\Delta_1$  as for the  $E_1$ ,  $E_1 + \Delta_1$  peaks. This indicates that the  $E_1'$ ,  $E_1' + \Delta_1$  splitting is due to the spin-orbit splitting of the  $L_3$  valence band, the splitting of the  $L_3$  conduction band being much smaller, as indicated by recent calculations for germanium.<sup>18</sup> The  $E_1'$ ,  $E_1' + \Delta_1$  splitting seems to be much larger than the  $L_3$  valence band splitting in CdTe and HgTe. This is also the case in<sup>14</sup> InAs and might be due to a non-negligible spin-orbit splitting at the  $L_3$ -conduction band or to other transitions superimposed onto the  $L_3-L_3$  transitions.

In the III-V compounds, the  $d$  electrons of the metal are separated from the valence electrons by about  $10 \text{ eV}$ .

<sup>13</sup> F. Lukeš, in *Proceedings of the 1962 International Conference on the Physics of Semiconductors, Exeter*, edited by A. C. Stickland (The Institute of Physics and Physical Society, London, 1962).

<sup>14</sup> H. Ehrenreich, H. R. Philipp, and J. C. Phillips, *Phys. Rev. Letters* **8**, 59 (1962).

<sup>15</sup> B. Segall (to be published).

<sup>16</sup> D. T. F. Marple and H. Ehrenreich, *Phys. Rev. Letters* **8**, 87 (1962).

<sup>17</sup> D. G. Thomas, *Suppl. J. Appl. Phys.* **32**, 2298 (1961).

<sup>18</sup> J. C. Phillips and L. Liu, *Phys. Rev. Letters* **8**, 94 (1962).

However, in the I-VII materials the  $d$  electrons of the metal are very heavily mixed with the outer electrons of the halogen and must be treated as valence electrons. The II-VI compounds represent an intermediate situation. The  $s$  valence electrons, largely from  $s$  electrons of the Group VI atom, lie about 10 eV below the top of the valence band. The  $d$  electrons of the metal are at about the same energy, hence, admixture of these atomic states is to be expected in the solid. In band calculations the  $d$  electrons of the metal must be treated as valence electrons. The  $d_1-d_2$  structure seen in Fig. 5 is very probably due to transitions from  $d$  electron levels to the conduction band. The  $d_2$  peak looks very similar to the peak observed by Philipp and Ehrenreich<sup>19</sup> in the III-V compounds at 22 eV and attributed to the same mechanism. The  $d_1$  peaks could be due to transitions from the same valence states to a different conduction band or to a splitting of the  $d$  states by the admixture of  $s$  electrons of the group VI atom.

The  $d_1$  and  $d_2$  peaks in HgTe occur at considerably lower energy than in CdTe and ZnTe since the energy separation between the  $d$  levels and the next  $s$  levels is also lower in Hg ( $\sim 9$  eV) than in Cd (12 eV) and Zn (11 eV). The  $d_1$  and  $d_2$  peaks have also been observed in II-VI compounds with wurtzite structure (ZnS, CdS, CdSe) at approximately the same energies.

#### GENERAL SYSTEMATICS

The concept of a perturbation parameter  $\lambda$ , correlating the energy gaps of diamond and zincblende semiconductors in the same electronic sequence, was introduced by Herman.<sup>20</sup>  $\lambda$ , which is a measure of the degree of polarity for one member of a sequence, is taken to be 0 for the Group IV materials, 1 for III-V materials, 2 for II-VI materials and 3 for I-VII materials. It has been shown<sup>6</sup> that the polar gap plotted against  $\lambda^2$  for one sequence gives a straight line, provided that the perturbation due to the polar potential is small compared with the gap between interacting states. This does not hold for the II-VI compounds when the states that form the gap interact via the polar potential ( $\Gamma_{15}-\Gamma_{15}$  and  $L_3-L_3$  gaps), in this case the  $\lambda^2$  dependence can be generalized to<sup>11</sup>:

$$E_p = E_{np} \left[ 1 + \frac{4\lambda^2 |\langle V_p \rangle|^2}{E_{np}^2} \right]^{1/2}, \quad (1)$$

where  $E_p$  and  $E_{np}$  are the gaps in the polar and nonpolar compound of the same isoelectronic sequence, respectively, and  $\lambda^2 |\langle V_p \rangle|^2$  the matrix element of the perturbing polar potential between the two states forming the gap. Figures 6 and 7 show the room-temperature  $\Lambda_3-\Lambda_1$ ,  $\Gamma_{15}-\Gamma_{15}$ ,  $X_5-X_1$  gaps plotted against  $\lambda^2$  for the horizontal sequences  $\alpha$ -Sn, InSb, CdTe, AgI and the skew sequence GeSn, GaSb, ZnTe, CuI. The points are

<sup>19</sup> H. R. Philipp and H. Ehrenreich, Phys. Rev. Letters **8**, 92 (1962).

<sup>20</sup> F. Herman, J. Electronics **1**, 103 (1955).

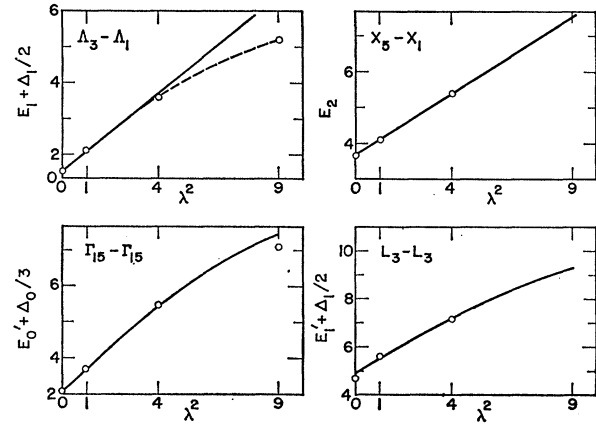


FIG. 6. Energy gaps for the horizontal sequence  $\alpha$ -Sn, InSb, CdTe, AgI.

experimental, and the solid lines calculated using Eq. (1) for the  $L_3-L_3$  and  $\Gamma_{15}-\Gamma_{15}$  gaps. Straight lines have been plotted for the  $\Lambda_3-\Lambda_1$  and  $X_5-X_1$  gaps. Values for the  $L_3-L_3$  gaps and the gaps of CuI and AgI have been taken from data obtained by Ehrenreich, Philipp, and Phillips<sup>14</sup> and Cardona.<sup>11</sup> Where gaps are perturbed by spin-orbit interaction, i.e., those transitions involving the  $\Lambda_3$  valence band, the energy of the unperturbed valence band has been taken. It has been assumed that spin-orbit effects raise the valence band by  $\Delta_0/3$  (where  $\Delta_0$  is the spin-orbit splitting at the zone center) from the unperturbed value.<sup>6</sup> The good agreement between the experimental points and the plotted lines confirms our interpretation. The deviation for the  $E_1$  gaps at  $\lambda=3$  has been discussed elsewhere.<sup>11</sup>

#### ESTIMATE OF EFFECTIVE MASSES

Effective masses at the various band extrema can be calculated by the  $\mathbf{k}\cdot\mathbf{p}$  method.<sup>21</sup> It has been pointed out by several authors<sup>6,22</sup> that the matrix elements of  $\mathbf{p}$  are the same for all semiconductors of the zincblende family. In the diamond-type materials, the effective mass at the bottom of the conduction band  $m^*(\Gamma_{2'})$  is mostly determined by the interaction with  $\Gamma_{25'}$  valence band. In a zincblende-type material the  $\Gamma_{25'}$  becomes  $\Gamma_{15}$  and the  $\Gamma_{2'}$  becomes  $\Gamma_1$  due to the lack of inversion symmetry and both the top of the valence band and the  $\Gamma_{15}$  conduction band have nonvanishing matrix elements of  $\mathbf{p}$  with the  $\Gamma_1$  conduction band. If we assume that the  $\Gamma_{2'}$  state does not mix with any other states under the action of the polar potential (all interacting states are indeed very far away), it is possible to handle the polar potential as done in Eq. (1) and derive the wave functions of the  $\Gamma_{15}$  valence band and the  $\Gamma_{15}$  conduction band as a function of the corresponding wave function of the nonpolar material belonging to the same isoelectronic sequence.

<sup>21</sup> E. Kane, J. Phys. Chem. Solids **1**, 82 (1956).

<sup>22</sup> H. Ehrenreich, Suppl. J. Appl. Phys. **32**, 2155 (1961).

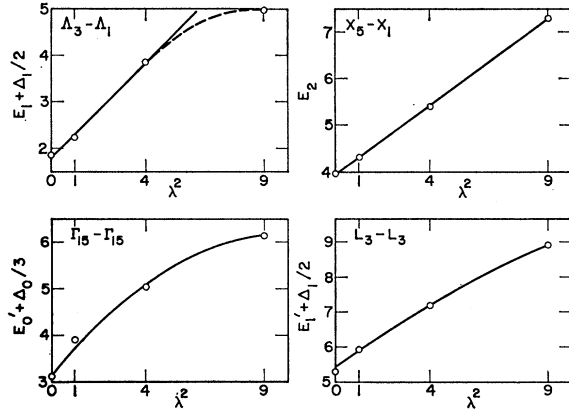


FIG. 7. Energy gaps for the skew sequence ( $\alpha$ -Sn-Ge), GaSb, ZnTe, CuI.

We can now calculate the  $\mathbf{k} \cdot \mathbf{p}$  terms between the  $\Gamma_1$  conduction band and both  $\Gamma_{15}$  bands. Neglecting spin-orbit splitting we obtain

$$\frac{m}{m^*(\Gamma_1)} = 1 + \left[ \frac{E_{p0}' + E_0'}{E_{p0}} \frac{E_{p0}' - E_0'}{E_{p0}' - E_{p0}} \right] \frac{P^2}{2E_{p0}'}, \quad (2)$$

where  $E_{p0}'$  and  $E_0'$  are the  $\Gamma_{15}-\Gamma_{15}$  gaps for the polar and the nonpolar material, respectively,  $E_{p0}$  and  $E_0$  are the  $\Gamma_{15}-\Gamma_1$  gaps and  $P$  is proportional to the matrix element of  $\mathbf{p}$  in the nonpolar material. The energies in Eq. (2) are at 0°K. They are approximately equal to the energies at 77°K. Spin-orbit splitting effects can be easily taken into account by increasing each gap by  $\Delta_0/3$  (for  $E_0 > \Delta_0$ ). If the polar perturbation is small, Eq. (2) reduces to the well-known expression

$$\frac{m}{m^*} = 1 + \frac{P^2}{E_{p0}}. \quad (3)$$

Ehrenreich<sup>22</sup> fitted the effective masses of all the III-V compounds with Eq. (3). He needed however a value of  $P^2 = 20$  eV, considerably smaller than for germanium ( $P^2 = 25$  eV). By using Eq. (1), the known values of  $m^*(\Gamma_1)$ , and the various energy gaps for the III-V compounds we obtain  $P^2 = 23$  eV, quite close to the value calculated for germanium. Using this value of  $P^2$  we can calculate  $m^*(\Gamma_1)$  for ZnTe and CdTe by using Eq. (2) and Table I. We obtain, for  $P^2 = 23$  eV,  $m^*(\Gamma_1)$

$= 0.16m$  for ZnTe,  $m^*(\Gamma_1) = 0.10m$  for CdTe.  $m^*(\Gamma_1)$  for CdTe is in excellent agreement with the value found experimentally ( $m^* = 0.11m$ ).<sup>23</sup> Equation (2) can also be used for wurtzite-type materials.<sup>24</sup> For CdS we obtain  $m^*(\Gamma_1) = 0.17m$  and for CdSe  $0.12m$ , in good agreement with the experimentally determined values,  $0.20m$  for<sup>25</sup> CdS and  $0.13m$  for<sup>26</sup> CdSe.

A similar treatment yields the valence band parameters<sup>27</sup>  $F$  and  $M$ :

$$F = \frac{E_{p0}' + E_0'}{2E_{p0}'} \frac{P^2}{E_{p0}}, \quad (4)$$

$$M \approx H_1 = \left( \frac{E_0'}{E_{p0}'} \right)^2 \frac{P^2(M_1)}{E_{p0}'},$$

where  $P^2$  is the same as in Eq. (1) and  $P^2(M_1) \approx 15$  eV (determined from the germanium parameters).

An expression similar to Eq. (2) can also be used to determine the transverse effective mass at the  $L_1$  point. In order to do this we must substitute  $E_0$  by the  $L_3-L_1$  gap, (approx. equal to  $E_1$ )  $E_0'$  by  $E_1'$  and the matrix element  $P^2 = 25$  eV.<sup>6</sup>

*Note added in proof.* Scouler and Wright [Bull. Am. Phys. Soc. **8**, 246 (1963)], have measured the reflectivity of HgTe at 12°K and found a splitting of the  $E_1' + \Delta_1$  peak reported in this paper. The splitting is 0.75 eV and, hence, it seems due to the spin-orbit splitting of the  $L_{3V}$  state ( $\Delta_1$ ). The  $E_1'$  peak does not split at low temperatures; it may be due to the spin-orbit splitting of the  $L_{3C}$  band. If the spin-orbit splitting of  $L_{3C}$  and  $L_{3V}$  are approximately the same, transition between these states should produce a triple peak (possibly  $E_1$  and the  $E_1' + \Delta_1$  doublet).

#### ACKNOWLEDGMENT

We should like to thank Oleh Tkál for performing some of the measurements.

<sup>23</sup> B. Segall, M. R. Lorenz, and R. E. Halsted, Bull. Am. Phys. Soc. **7**, 544 (1962).

<sup>24</sup> M. Cardona, Phys. Rev. **129**, 1068 (1963).

<sup>25</sup> W. W. Piper and D. T. F. Marple, Suppl. J. Appl. Phys. **32**, 2237S (1961).

<sup>26</sup> J. O. Dimmock and R. G. Wheeler, Suppl. J. Appl. Phys. **32**, 2271S (1961).

<sup>27</sup> G. Dresselhaus, A. F. Kip, and C. Kittel, Phys. Rev. **98**, 368 (1955).